FATIGUE ANALYSIS OF CONROD BEARING

J-L. Ligier, L. Dutfoy

Powertrain Division, RENAULT SAS, 67 rue des Bons Raisins, 92508 Rueil-Malmaison Cedex, France

1) Abstract

For many years, bearing suppliers use efficiently the specific pressure to evaluate the fatigue risk of conrod bearings. However, modern engines have made the bearing more sensitive to various phenomena such as the thermal expansion or the elasticity of the conrod housing. These effects modify the stresses in the bearing layers and by the way the fatigue loading. In this paper, we analyze the elastic and plastic behavior of the bearing during the engine life. We detail and provide the analytical relationships, which determine stresses in the overlay and the substrate of the bearing. Various loadings are taken into account such as the thermal loading, the hydrodynamic pressure field, the fitting loading, the free spread loading.

The knowledge of the relationships helps to understand the mechanical behavior of the bearing. Particularly, it allows demonstrating that plastic flow occurs in the substrate and in the overlay during the first combustion cycles and the first thermal cycles. Residual stresses are introduced by plastic flow and modify the stress tensor in the different layers. Therefore, the two layers are subject to high cycles fatigue (H.C.F.) with combustion cycles and low cycles fatigue (L.C.F.) with thermal loading. The high cycle fatigue analysis is performed with multiaxial criteria.

2) Introduction

From a general point of view, we could say that the bearing behavior is quite complex and several mechanical questions are not yet clearly solved. One of the recurrent questions could be: how a lead overlay can withstand a hydrodynamic pressure of 200 MPa as its specific strength is lower than 20 MPa at 150 °C. In addition of these understanding weaknesses which have influence on the bearing design robustness, modern bearing applications are becoming more and more severe in terms of specific pressure, minimum oil film thickness. For example, specific pressure (diametral pressure) can reach more than 110 MPa on turbo diesel conrod bearing. Also, mixed lubrication appears currently in conrod bearing simulation and is observed from the field.

These two previous aspects involve for the design engineer, that:

- bearing optimization design for new powerful engine will be very delicate, as bearing behavior is not fully understood,
- design modification will be difficult to evaluate in terms of bearing stress or strain to check its reliability with respect to fatigue, wear, seizure…,
- bearing sensitivity to design parameters such as free spread, circumferential length, and thickness of the substrate is also difficult to estimate. By the way, it does not allow defining which process or machining parameter needs accurate control on its dispersion.

In automotive industry, it is quite common today to perform many numerical simulations in order to design and validate engine components and more particularly bearing and its lubrication circuit. For this last kind of simulation, the most refined and efficient tools are elasto-hydrodynamics finite element code as Accel, Excite [1,2]. However, for obvious reasons of calculation time consumption, the finite element meshes of these kinds of calculation are quite crude. For example, the bearing and the conrod form a single body. The finite element size in the bore is around 5 mm. Generally, just one distorted element (1.5 mm thick 5 mm wide) is used to represent the bearing thickness. With linear elastic behavior of the bearing and such mesh, it is impossible to predict realistic stresses in the substrate and in the overlay of the bearing. The major and realistic result obtained from the elastohydrodynamic tool is the fluid pressure on the bearing surface. This one can be used as an input data for non-linear calculation of the conrod fitted with bearing.

Experience from the field has conducted bearing suppliers to propose different materials and structures. The most common structures are given on figure 1. One of the structures, called bimaterial bearing, on the right part of the figure, is mainly made with the steel back and the antifriction substrate. An intermediate layer (40 µm thick) does the bonding between these two parts. The second type of structure, or trimetallic bearing, is composed of three parts: the bearing back in steel (sometime in copper alloy), the substrate, and the overlay. We will consider indifferently these two kinds of structure.

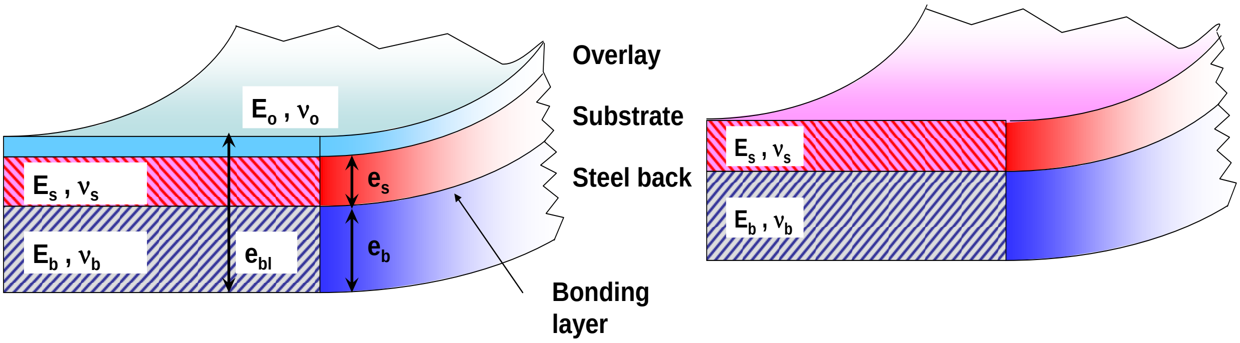

Figure 1: Bearing structure

In this analysis, to differentiate the different components, we add a suffix; b, s, o, lay, h respectively steel back, substrate, overlay, layers on the steel back (substrate or overlay), housing for geometrical and material characteristics and superscript letters for stress and strain variables.

Concerning the bearing reliability, most of the bearing suppliers used the specific pressure to determine the fatigue resistance of bearing with respect to bearing material and bearing application (type and size). No simulation to estimate bearing stress is done by bearing suppliers or can be found in the literature. It does not allow to evaluate the fatigue resistance with respect to fatigue criteria as Goodman, Haigh, Sines, Dang Van criteria [3]. On figure 2, a fatigue damage example is presented and is sometimes called “fatigue pitting” [4].

Figure 2: Lead-tin-copper overlay fatigue

As one of the current targets is to perform fatigue analysis, it is necessary to detail the stress tensor in the different bearing layers. Several phenomena generate stresses in the bearing layers, substrate and overlay as for example the bearing shaping, the operating condition.
A global overview of the stress origins is given on table1. In this table, several aspects are

considered: the nature of the loading (constant, low frequency, high frequency), the stress relaxation effect and the stress level. Stress relaxation is a delicate item related to the exposure time and the material. For overlays like lead alloy, tin alloy, sputtered aluminum alloy, we have considered that stress relaxation occurs after few hours at high temperature in the worst case [150 – 200 °C] [5-8]. For this range of temperature, creep is activated for all these kinds of materials. For copper alloy substrate and aluminium alloy substrate the residual stresses must be taken into account.

Stress origin		**Const**	**Low freq.**	**High freq.**	**Relax**	**Level**	**Comment**
Housing deformation	Overall		**X**			**+**	
	Local		**X**			**-**	Ex: Bolt hole effect
Fitting	Interference fitting	**X**				**+**	
	Free spread	**X**				**+**	
	Friction	**X**			**X**	**-**	Vanishing after few cycles
Thermal	Local circonf.		**X**			**+**	
	Overall		**X**			**+++**	Cold engine to warm engine
	Radial gradient		**X**			**-**	Negligible, <<1°C/mm
Residual		**X**			**X**	**+**	Thermal treatment or shaping
Hydro. Pressure				**X**		**+++**	

Table 1 : Bearing stress overview

These different sources of stress are going to be examined in the following chapters.

3) Main simplifications and hypothesis

Before writing the various stress expressions, it is necessary to adopt several hypothesis and simplification to solve more easily this problem. Therefore, we will assume that:

- The different bearings layers are perfectly bonded and the fatigue does not initiate in the bonding interface but is due to high stress level in the layer bulk.
- The behavior of the bearing back and the layers is assumed elastic and perfectly plastic (no hardening).
- The conrod housing behaves as a "master" with respect to the bearing except when the problem can be solved easily without this simplification. This can be justified by the different thicknesses of these two components [9].
- The layer (substrate or overlay) behaves as a "slave" with respect to the steel back of the bearing which is then the "master" [9].
- Due to the small thickness of the layers with respect to the bearing back, the housing and the curvature radius, we consider at first that the stress is uniform with respect to the bearing thickness except for specific bending of the bearing. It means that no shear stress exists in the thickness. Curvature effect is also neglected.
- The hydrodynamic pressure can be approximated by a power law in x^2 with respect to the circumferential length and by a power law in z^6 with respect to the width.
- The bearing can slip locally in its housing and does not constitute a single body with the conrod housing as it is often assumed in simulation. The slippage helps a lot to simplify analytical relationship.

Due to the importance of the last two assumptions, some details are given below.

Hydrodynamic pressure approximation

To analyze the fatigue of the conrod bearing device, it is necessary to estimate the internal stress in the bearing for the highest loading. The most important factors for fatigue are the pressure gradient and the maximum pressure. So, we will focus our analysis in the crown of the upper conrod bearing when the load and the temperature are maximum. A realistic pressure field is given on figure 3 [10]. This field was obtained with EHL calculation for a turbocharged Diesel engine. The maximum pressure is approximately 250 MPa.

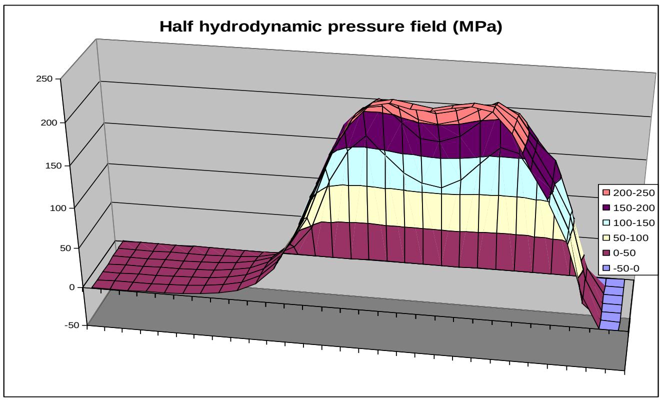

Figure 3 : Hydrodynamic pressure field

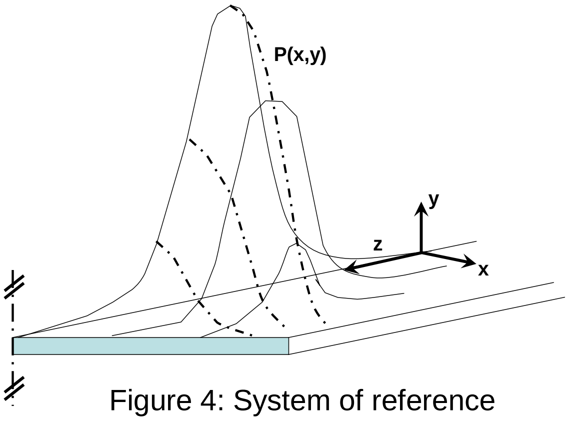

Figure 4: System of reference

For this specific area, we can approximate the pressure by the following relationship:

$P_h(x,z) = P_{max}\left(1-\left(\frac{x}{a}\right)^2\right)\left(1-\left(\frac{z}{b}\right)^6\right)$ where P_{max} is the maximum hydrodynamic pressure, b the half width of the bearing and "a" a certain length in the circumferential direction with the conventions mentioned on figure 4. Due to elasticity of the housing, the value "a" is linked with the conrod shank size.

Under such pressure field, we can observe in the z direction, the pressure is uniform except near the bearing faces. Also, we suppose the determination of the bearing stress and the conrod stress can be considered as a plane strain elasticity problem. This is particularly suitable when we look at point located near bearing shell.

For this plane problem, we assume that the conrod body behaves like a plane (2ax2h). The height "h" represents a certain height of the conrod body. Due to the fitting condition, the bearing follows the deformation of the conrod. Then, the question is: does the bearing slip in its housing?

Bearing slippage

For a bearing part subjected to hydrodynamic pressure, the bearing has two ways to behave as described on figure 5.

On figure 5, we can see that one part of the interface between the bearing and the housing is slipping whereas the other part is perfectly bonded. To determine the slipping area size we can look at the simplified model on figure 6, which represents a slice of the bearing slipping on the elastic housing. The loading is done by the previous hydrodynamic pressure field and is supposed to be uniform in the z direction.

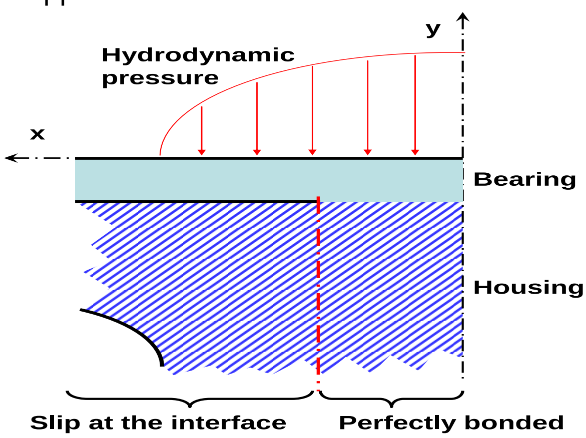

Figure 5: Bearing bonding

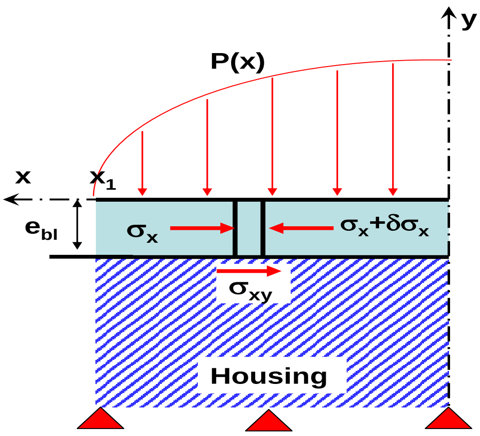

Figure 6: Slip equilibrium

The force equilibrium for a very small element (figure 5) gives with the notation of the figure, the following relationship: $e_{bl}\dfrac{d\sigma_x}{dx}=\sigma_{xy}$.

With the hypothesis the slipping obeys to Coulomb's friction law, we get, for the normal stresses : σ_x σ_y, and the shear stress at the surface : σ_{xy} , after integration and taking into account that $\sigma_x(a)=0$: $\sigma_x(x)=\dfrac{\varphi}{e_{bl}}\int_x^a P(\zeta)d\zeta$; $\sigma_{xy}(x)=-\varphi P_h(x,0)$ with φ friction coefficient, $\sigma_y(x)=-P_h(x,0)$.

In the case of a perfect bonding, the bearing can be considered as a part of the conrod. With the knowledge of the stress in the single body (conrod + bearing), the bonding, located at ($y=h-e_{bl}$), will be considered as perfect if the shear stress in this body at the interface between the bearing and the housing is lower than the previous shear stress $\sigma_{xy}(x)$. It means: $\sigma_{xy}(x,h-e_{bl})\le|\varphi P_h(x,0)|$

An expression of $\sigma_{xy}(x,h-e_{bl})$ can be obtained by the least work principle applied on the following Airy function, Φ, [11]

$\Phi(x,y)=P_{\max}\dfrac{x^2}{2}\left(1-\dfrac{1}{6}\left(\dfrac{x}{a}\right)^2\right)+\left(y^2-b^2\right)^2\left(x^2-a^2\right)^2\left(k_1+k_2x^2+k_3y^2\right)$ and k_i determined with $\dfrac{\partial V_c}{\partial k_i}=0$ and $V_c=\iint\left((\Phi_{,xx})^2+(\Phi_{,yy})^2+2(\Phi_{,xy})^2\right)dxdy$.

With this Airy function, we have the standard relationships: $\sigma_x=\dfrac{\partial^2\Phi}{\partial y^2};\sigma_y=\dfrac{\partial^2\Phi}{\partial x^2};\sigma_{xy}=-\dfrac{\partial^2\Phi}{\partial x\partial y};$

The determination of the constants k_i do not present difficulties with software like Maple [12] but the expressions are too long to be written here. After calculation and considering the bearing thickness as a variable, we obtain figure 7, describing the shear stress difference between the internal stress and the friction shear stress. When the result is negative (below the black line), it means that there is slippage. Figure 7 shows that slippage happens for various values of x and for quite thin bearing shell. Below in the text, we will consider that the bearing slips in its housing during pressure loading.

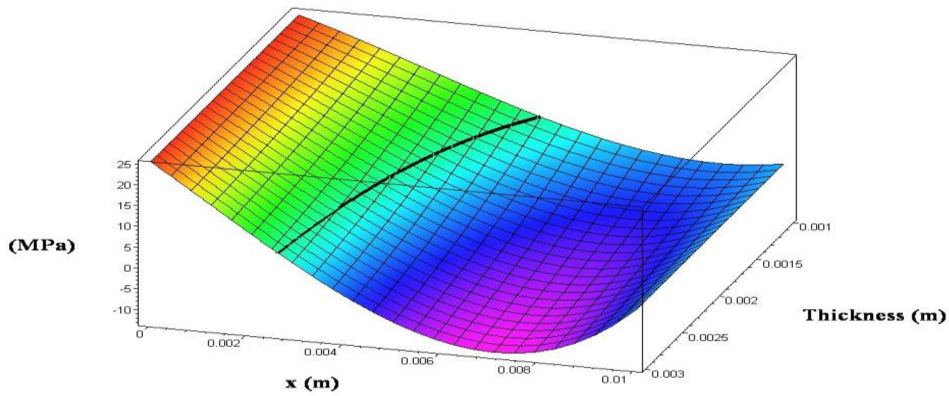

Figure 7: Shear stress difference

4) Stress analysis

As mentioned in table 1, several phenomena generate stresses in the bearing and particularly in the substrate or the overlay. Following the order of table 1, the various stress origins are:

Overall Housing distortion stress

The stresses in the bearing layers due to the housing distortion are analyzed when the load is applied in the conrod body direction. With Elastohydrodynamic calculation, we know that the oil film is very thin in the loaded area. It means that the bearing and the conrod are wrapped around the shaft. Due to the load direction there is no significant housing elongation and by the way, no interference fit modification.
For a bearing with a radial clearance C_r, and an inner radius R_i, we can estimate the stress in the overlay bearing. Thanks to the slippage between the bearing and the housing, the stress generated by the housing distortion is the normal stress σ_x. With bending relationships, the stress tensor is:

$$\begin{cases} \sigma_x = y_{nf} E_{lay}\left(\dfrac{1}{R_i} - \dfrac{1}{R_i - C_r}\right) \\ \sigma_y = \sigma_z = \sigma_{xy} = \sigma_{yz} = \sigma_{zx} = 0 \end{cases}$$

with y_{nf} the location of the considered fiber in the layer with respect to the neutral fiber of the global bearing. The neutral fiber location with respect to the symmetry thickness is : $\dfrac{e_{bl}}{2} - e_s + \dfrac{e_s^2 E_s - e_b^2 E_b}{2 e_b E_b + e_s E_s}$

For a quick evaluation, we can consider that for the surface $y_{nf} = e_{bl}/2$ with e_{bl} the bearing thickness

Local housing distortion stress

In the crown conrod area where our analysis is focused, the local distortion is negligible. In the axial bearing direction, the housing bore distortion is smaller than 0.3 µm for the highest loaded bearing (Pressure max: 250 MPa). With common automotive conrods, no specific bore feature introduces strain or stress variation.

Fitting interference stress

To get a certain contact pressure between the bearing and the housing, the bearing has a circumferential length greater than its housing. The extra length is called ΔL (for the two half bearings). To fit the bearing, it is necessary to apply a certain compressive circumferential stress in the bearing. This kind of stress vanishes in the overlay during the engine life. If we consider the bearing and the conrod housing as thin shells, the interference ΔL generates the following stress tensor in the bearing layer:

$$\begin{cases} \sigma_x = -\dfrac{\Delta L}{\pi D} E_{lay}\left(\dfrac{e_h E_h}{e_h E_h + e_{bl} E_{bl}}\right) \\ \sigma_y = \sigma_z = \sigma_{xy} = \sigma_{yz} = \sigma_{zx} = 0 \\ with \quad \mathrm{E_{bl}} = \dfrac{e_{lay} E_{lay} + e_b E_b}{e_{lay} + e_b} \end{cases}$$

Free spread stress

At free state, the bearing has a diameter greater than its housing. This extra diameter is called ΔD. During the fitting process, the diameter reduction is due to force reaction at the edges of the housing. These reactions generate bending stresses in the bearing. This kind of stress is permanent in the substrate. For the overlay, the free spread stress disappears with the relaxation effect. With Strength of Material theory, we simply obtained the following relationship for the stress tensor in the overlay:

$$\begin{cases} \sigma_x = -\dfrac{8\Delta D}{\pi D^2}\dfrac{EI_{bend}}{I_{bend}}\cos(\theta)y_{nf} \\ \sigma_y = \sigma_z = \sigma_{xy} = \sigma_{yz} = \sigma_{zx} = 0 \\ EI_{bend} = \int_{e_{bl}} E(y_{nf})y_{nf}{}^2 dy_{nf} \quad \text{et } \mathrm{I_{bend}} = \int_{e_{bl}} \dfrac{E(y_{nf})}{E_b} y_{nf}{}^2 dy_{nf} \end{cases}$$

In this relationship, θ is measured from the joint face of the bearing and y_{nf} is evaluated from the neutral fiber [13]

Friction fitting stress

During the fitting bearing process, friction is generated at the interface between the bearing and the housing. Nevertheless, as the housing is distorted during each engine cycle, the friction stress vanishes quite rapidly. By the way, it is not necessary to consider it after few cycles.

Global thermal stress

This the most important contributor in terms of shear stress. The substrate and the overlay have, for all bearing design, higher thermal expansion than the steel back of the bearing (except for copper back). As soon as the temperature increases in the bearing from the manufacturing temperature or a certain reference temperature, T_{ref}, up to the local operating temperature T_{op}, compressive thermal stresses are generated. The general relationships for thermal strains in a thin layer are [14]:

$$\begin{cases} \varepsilon_x = \dfrac{\sigma_{xx}(1-\nu)}{E} + \alpha(T_{op} - T_{ref}) \ ; \ \varepsilon_y = +\alpha(T_{op} - T_{ref}) \\ \varepsilon_z = \varepsilon_x \ ; \ \varepsilon_{xy} = \varepsilon_{yz} = \varepsilon_{zx} = 0 \end{cases}$$

As the substrate or the overlay, identified with the sign "lay", must have the same strain than the bearing back, it involve that for thin structure, the equations to solve are:

$$\varepsilon_x{}^b = \varepsilon_x{}^{lay} \quad \text{and} \quad \mathrm{e_b}\sigma_x{}^b + \mathrm{e_{lay}}\sigma_x{}^{lay} = 0$$

After calculations, we obtain that the thermal stress tensor, in the substrate or the overlay, is:

$$\begin{cases} \sigma_x^{lay} = \sigma_z^{lay} = \dfrac{e_{lay}(\alpha_b - \alpha_{lay})E_b E_{lay}(T_{op} - T_{ref})}{e_b E_b(1-\nu_{lay}) + e_{lay}E_{lay}(1-\nu_b)} \\ \sigma_y^{lay} = \sigma_{xy}^{lay} = \sigma_{yz}^{lay} = \sigma_{zx}^{lay} = 0 \end{cases}$$

If we consider that the layer has a "slave behavior" with respect to the bearing back, which becomes the "master", the previous relationships are simpler:

$$\begin{cases} \sigma_x^{lay} = \sigma_z^{lay} = \dfrac{(\alpha_b - \alpha_{lay})E_{lay}(T_{op} - T_{ref})}{(1-\nu_{lay})} \\ \sigma_y^{lay} = \sigma_{xy}^{lay} = \sigma_{yz}^{lay} = \sigma_{zx}^{lay} = 0 \end{cases}$$

To illustrate the importance of this stress, we consider the following numerical application:
T_{ref}=20°C; T_{op}=150°C; α_b=1,1 10^{-5}°C^{-1}; α_{lay}=2,2 10^{-5}°C^{-1}; E_b=2,1 10^5 MPa; E_{lay}=7 10^4 MPa; ν_b=0,27 ; ν_{lay}=0,33;
Exact formula : $\sigma_z^{lay} = 149\,\mathrm{MPa}$ Approximated formula : $\sigma_z^{lay} = 140\,\mathrm{MPa}$

Local and radial thermal stress

The temperature varies along the circumference but in the crown area, the temperature variations are not so important when there is no high direct contact between the shaft and the bearing overlay [15]. The thermal circumferential gradient is less than 1°C/mm and is not sufficient to generate new significant stress with respect to the previous thermal stress

estimation. For this analysis, we will neglect this aspect.
For the radial direction the gradient is very small, less than 1°C in the bearing thickness [16]. This is due to the poorness of the heat transfer between the conrod and the surrounding air. We will also neglect this aspect.

Residual stress
The main part of the residual stress concerns the substrate, which is present during the bearing shaping. For automotive engine bearing, the shaping process involves plastic deformation of the bilayer metal strip, which constitutes the bearing. The maximum bending strain ε_{bend} is $\varepsilon_{bend} \approx \frac{e_{bl}}{D}$. With common bearing design $\varepsilon_{bend} \equiv 4/100$ which implies a high level of plasticity during the shaping. If the bearing materials have pure plastic behavior, the residual stress tensor in the substrate is:

$$\begin{cases} \sigma_x^{lay} = \mathrm{Re}_{lay} - y_{nf} \dfrac{M_{pla}}{I_{bend}} \dfrac{E_{lay}}{E_b} \text{ and} \\ \sigma_y^{lay} = \sigma_z^{lay} = \sigma_{xy}^{lay} = \sigma_{yz}^{lay} = \sigma_{zx}^{lay} = 0 \end{cases} \quad M_{pla} = \mathrm{Re}_b \left(\frac{\left(\frac{e_b}{2} - \frac{e_{lay}}{2}\right)^2}{2} - e_{lay}^2 \frac{(\mathrm{Re}_{lay} - \mathrm{Re}_b)^2}{8\,\mathrm{Re}_b^2} \right) + \mathrm{Re}_{lay} \left(\frac{\left(\frac{e_b}{2} + \frac{e_{lay}}{2}\right)^2}{2} - \frac{\left(\frac{e_b}{2} - \frac{e_{lay}}{2}\right)^2}{2} \right)$$

With Re_b, Re_{lay} : Yield strength of the bearing back and the substrate.

Hydrodynamic pressure.
This is one of the most important stress contributors. To estimate the stress, we suppose that the bearing slips on the bearing surface. It means that the stress in the plane perpendicular to the loading direction can be supposed to be close to null. But, as the overlay and the substrate have lower Young's modulus than the body on which they are bonded the hydrostatic stress tensor is important.
The normal stress in the loading direction is: $\sigma_y = -P_h(x,z)$. Due to the hypothesis of a perfect bonding between the layers and the bearing support, we have to impose :

$$\varepsilon_x{}^b = \varepsilon_x{}^{lay}\,;\ \varepsilon_z{}^b = \varepsilon_z{}^{lay}\,;\ \varepsilon_x{}^b = \frac{\nu_b}{E_b} P_h(x,z) - \frac{\varphi}{E_b e_{bl}} \int_x^a P_h(\zeta,z)\,d\zeta$$

and $\varepsilon_z{}^b = \dfrac{\nu_b}{E_b} P_h(x,z) - \dfrac{\varphi}{E_b e_{bl}} \displaystyle\int_z^b P_h(x,\xi)\,d\xi$.

With the hypothesis the bearing back has a « master » behavior with respect to the layers, extra stresses are generated in the layers. The stress tensor in the layer becomes:

$$\begin{cases} \sigma_x^{lay} = \dfrac{E_{lay}}{(1-\nu_{lay})} \left(\dfrac{\nu_b}{E_b} - \dfrac{\nu_{lay}}{E_{lay}} \right) P_h(x,z)) - \dfrac{E_{lay} E_b}{(1-\nu_{lay}^2)} \left(\dfrac{\varphi}{E_b e_{bl}} \displaystyle\int_x^a P_h(\zeta,z)\,d\zeta + \dfrac{\nu_{lay}\varphi}{E_b e_{bl}} \displaystyle\int_z^b P_h(x,\xi,)\,d\xi \right) \\ \sigma_y^{lay} = -P_h(x,z); \\ \sigma_z^{lay} = \dfrac{E_{lay}}{(1-\nu_{lay})} \left(\dfrac{\nu_b}{E_b} - \dfrac{\nu_{lay}}{E_{lay}} \right) P_h(x,z)) - \dfrac{E_{lay} E_b}{(1-\nu_{lay}^2)} \left(\dfrac{\nu_{lay}\varphi}{E_b e_{bl}} \displaystyle\int_x^a P_h(\zeta,z)\,d\zeta + \dfrac{\varphi}{E_b e_{bl}} \displaystyle\int_z^b P_h(x,\xi)\,d\xi \right) \\ \sigma_{xy}^{lay} = \sigma_{yz}^{lay} = \sigma_{zx}^{lay} = 0 \end{cases}$$

5) Fatigue Analysis
Thanks to chapter 4, we know each stress contribution and can proceed to the fatigue analysis taking into account the relaxation effect which makes certain stresses disappear. Table 2 gives the overview on the kind of stress we have to consider to perform a fatigue analysis.

Stress origin	**Sit.**	**Substrate**			**Overlay**		
		Permanent	**H.C.F.**	**L.C.F.**	**Permanent**	**H.C.F.**	**L.C.F.**
Global Housing deformation	**1**	**-**	**X**	**-**	**-**	**X**	**-**
Fitting interference	**2**	**X**	**-**	**-**	**-**	**-**	**-**
Free spread	**3**	**X**	**-**	**-**	**-**	**-**	**-**
Global thermal	**4**	**X**	**-**	**X**	**-**	**-**	**X**
Residual stress	**5**	**X**	**-**	**-**	**-**	**-**	**-**
Hydrodynamic pressure	**6**	**-**	**X**	**-**	**-**	**X**	

Table 2: Stresses for the fatigue analysis

To analyze the fatigue we will use the following numerical data:
E_o=1,5 10^4 MPa; ν_o=0,47; α_o=2,3 10^{-5} °C^{-1}; e_o=0,015 mm;
E_s=6,7 10^4 MPa; ν_s=0,34; α_s=2,1 10^{-5} °C^{-1}; e_s=0,3mm;Re_s=80 MPa;
E_b=2,1 10^5 MPa; ν_b=0,3; α_b=1,1 10^{-5} °C^{-1}; e_b=2,2mm; Re_b = 250 MPa
E_h=2,1 10^5 MPa; ν_h=0,3; e_h=10mm;
Ri =25 mm; Cr= 25µm; ΔD=1mm; ΔL=0,1mm ;
T_{op} =150 °C; T_{ref} = 30°C; P_{max}= 200 MPa;

After calculation we got the results of table 3:

		Cold combustion cycles		**Hot combustion cycles**	
		No combustion	Combustion	No combustion	Combustion
Overlay	Cycle	0	1+6	4	1+4+6
	Von Mises stress	0	39 MPa	32 MPa	16 MPa
	Hydrostatic stress	0	-173 MPa	-21 MPa	-210 MPa
Substrate	Cycle	2+3+5	1+2+3+5+6	2+3+4+5	1+2+3+4+5+6
	Von Mises stress	52 MPa	85 MPa	136 MPa	56 MPa
	Hydrostatic stress	-17 MPa	-152 MPa	-85 MPa	-219 MPa

Table 3: Stress during combustion cycles

The main result is that for the different loading situations and for substrate and overlay, the specific Von Mises stress is higher than the yield strength of each layer. It involves that plastic flows will occur for the first combustion cycles and first thermal cycle as described on figure 8. At each plastic flow occurrence, residual stresses are generated. The important aspect is that plastic flows occur under high hydrostatic compression. This compression avoids crack propagation during the first cycles.

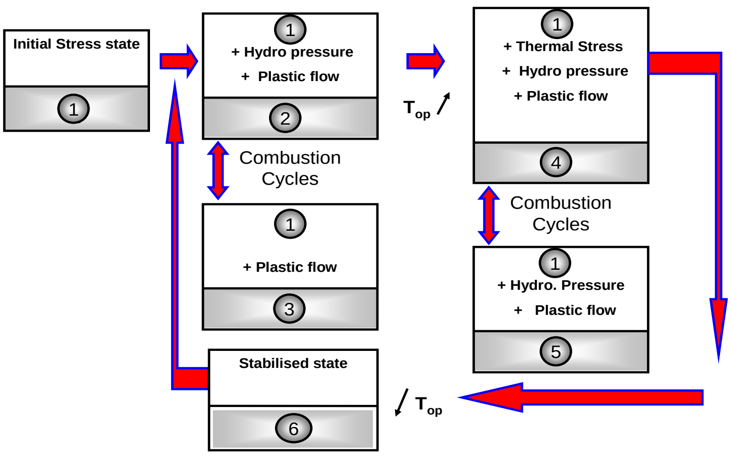

Figure 8: Loading cycle synopsis

As it appears on figure 8, the bearing must have resistance with respect to low cycle fatigue due to thermal evolution and to high cycle fatigue due to combustion loading. However, to estimate the fatigue resistance it is necessary to identify the residual stresses, which modify the previous results. At first, residual stress must allow the layer to operate in elastic regime during combustion cycle.

On figure 9, we plot the Von Mises stresses for the overlay for the hot combustion cycle. The stresses are evaluated with the introduction of residual stresses S1 and S3 applied on the normal stress $\sigma_x;\sigma_z$. As it appears on the figure, the two stress states must have a common area where the Von Mises is lower than the yield stress. This is the first condition to assure that the bearing overlay can operate correctly. By a certain way, it corresponds to the fact that bearing supplier considers specific pressure to assure the fatigue resistance. As residual stresses must minimize the deformation energy during each cycle, their location is in the center of the cone-shaped surface intersection. It is accelerated by the creep phenomena.

In the particular case of the overlay we found that S1=24 MPa and S3= 27 MPa. Taking into account these new stress values, we can perform the fatigue analysis of the overlay. Fatigue analysis is done with Dang Van criterion [3]. We consider two stress conditions with the tensor $\overline{\overline{\sigma_1}}$ et $\overline{\overline{\sigma_2}}$ respectively for overlay stresses with and without combustion.

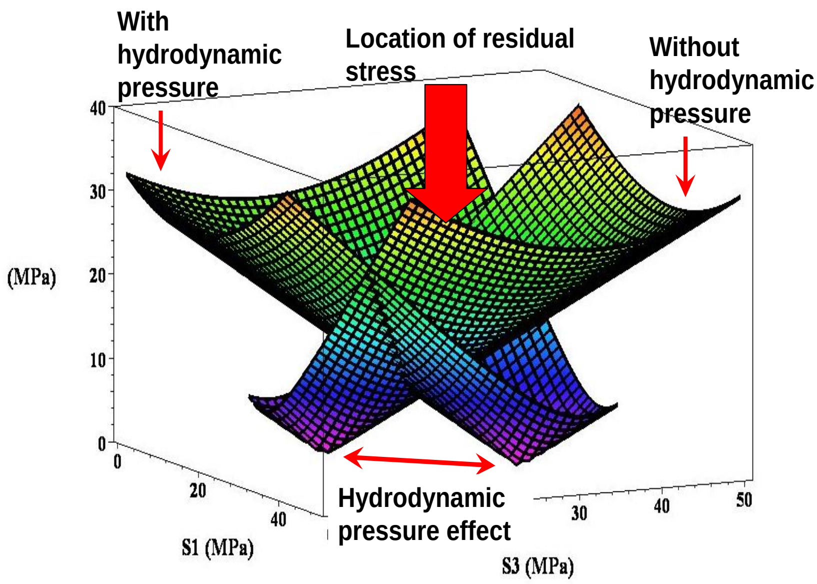

Figure 9: Residual stress

In the Dang Van graph, the horizontal axis is dedicated to the hydrostatic pressure $trace\overline{\overline{(\sigma_i)}}/3$ and maximum shear cission stress appears on the vertical axis. This shear stress is defined by:

$\tau_i = \frac{s_i^I - s_i^{III}}{2}$ with the stress tensor "s" defined by $\overline{\overline{s_i}} = \overline{\overline{S_i}} - \overline{\overline{C}}$ and "S" the deviatoric stress tensor and "C" the center of the hypersphere.

In the overlay case, we have plotted on figure 10 lines representing the engine cycle for cold and hot conditions. As the lines start from very low value of hydrostatic pressure we have not represented these parts of the curves.
With respect to the Dang Van criteria we can see that one point is critical and is cold situation with residual stress . But this cold situation is more a spirit view as the oil temperature is very seldom so cold.

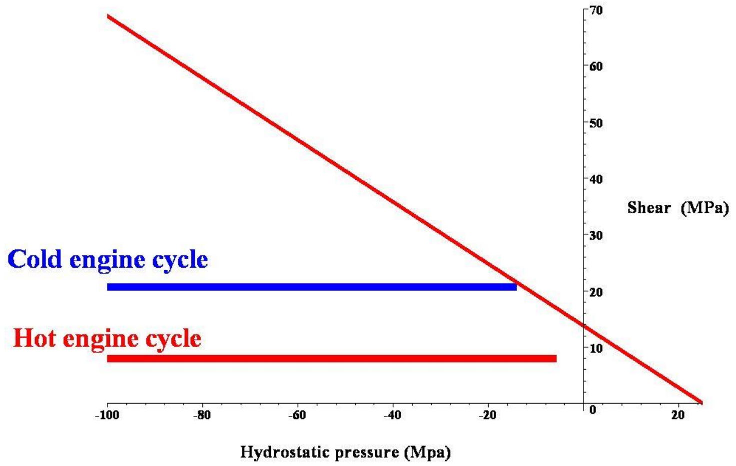

Figure 10 : Dang Van Diagram

The same analysis can be done on the substrate. For the both layers, which have quite similar behavior with respect to fatigue, sensitivity analysis provides the following results:

- The most influential parameter is the operating temperature, T_{op}, which increases the stress and reduces the yield strength. Thanks to the oil temperature limit in the engine, T_{op} does not vary a lot.
- The second most influential parameter is the hydrodynamic pressure. This one is controlled by the conrod shank size.
- The other parameters weakly sensitive are:
  the Young's modulus, the Poisson's ratio, the thermal expansion, the overlay thickness plays a role with respect to the yield strength like the relationship proposed by Suresh [9]: $\mathrm{Re}_o = \mathrm{Re}_{bulk}\left(\frac{cste}{e_o}+1\right)$
- The parameters quite non sensitive are:
  the substrate thickness,
  under normal conditions, the shaping process, fitting loading DD whose stress disappear with plastic flow,
  the radial clearance except the modification of the hydrodynamic pressure,
  the curvature radius.

6) Conclusion

Thanks to elasticity theory and Strength of Material theory analytical relationships for internal stress in the bearing have been written. With them, it has been possible to write the stress tensor in the overlay and the substrate of the bearing in the area where the hydrodynamic pressure exists.

For highly loaded bearing, it appears that plastic flow occur in the bearing layers for each loading cycle. It involves that the bearing has to resist to two kind of fatigue : low cycle fatigue due to thermal cycle and high cycle fatigue due to combustion cycle.

The fatigue sensitivity analysis reveals the predominant factors to improve the bearing resistance are yield strength, fatigue resistance, Poisson's ratio, thermal expansion coefficient.

The limit of the diametral pressure, used by bearing suppliers, is equivalent to constrain the maximum hydrodynamic pressure to allow the bearing layer to operate in elastic regime during combustion cycles.

7) Acknowledgements
The authors are indebted to Mr. Jean-Paul Cadalen (Renault SAS) for valuable discussions.

8) References

[1] Bonneau D. Lubrification EHD des Paliers de Moteurs Thermiques. Laboratoire de Mécanique des Solides . UMR6610. Poitiers

[2] Ma M.-T., Offner G., Loibnegger B., Priebsch H. H., A Fast Approach to Model Hydrodynamic Behaviour of Journal Bearings for Analysis of Crankshaft and Engine Dynamics**.** Transient Processes in Tribology, Proceedings of the 30th Leeds-Lyon Symposium on Tribology. Volume 43, Pages 3-872 (2003)

[3] Socie D. F., Marquis G. B., Multiaxial Fatigue. SAE international 2000

[4] Ligier J.-L., Avarie en Lubrification: Application aux Paliers. Editions Technip. 2004.

[5] Elsukova T.F. & al. Creep in Lead Alloys. Russian Physics Journal. Vol. 16, N°11, 1555-1558, 1974.

[6] El-Dlay A. A., & al. Transient Creep Characteristics in PB-Sn-Zn Ternary Alloys. Egypt J. Sol., Vol. 23, N°1, 2000.

[7] McCabe R. J., Fine M. E., The Creep Properties of Precipitation Strengthened Tin-Based Alloys. Journal of the Minerals, Metals and Materials Society. Vol. 52, N°6, 33-35, 2000.

[8] Dos Santos J.M.M.& al. Sensitivity of a Rotating Beam Sensor for Stress Evaluation in Aluminum Thin Films. Materials Science Forum. Vol. 490-491, pp 649-654, 2005.

[9] Freund L. B., Suresh S., Thin Film Materials. Cambridge University Press. 2003.

[10] Dutfoy L., Lubrification EHD de la tête de bielle. BMIR M062-2007-001 2.0, Internal Renault Report. 2007.

[11] Timoshenko S. P., Goodier HJ. N., Theory of Elasticity. McGraw-Hill International editions. 1970.

[12] Fishback E.P. Linear and Nonlinear Programming with MAPLE. CRC Press. 2009.

[13] Christensen R. M., Mechanics of Composite Materials. Krieger Publishing Company. 1991.

[14] Boley B. A. Weiner J. H., Theory of thermal stresses. John Wiley 1988.

[15] Boncompain R., Fillon M., Frene J., Effets Thermiques dans les paliers hydrodynamiques. Journal de Mécanique Théorique et Appliquée, Vol. 6, N°2, pp 253-293, 1987.

[16]. Ligier J.-L., Dutfoy L., Modeling and Prediction of Simplified Seizure Mechanism Occurring in Conrod Bearing. 2010. Workshop « Bearing Under Severe Operating Conditions », EDF-LMS FUTUROSCOPE. Poitiers.